Electron transport properties of ternary metallic glasses $(Ni_{33}Zr_{67})_{1-x}X_x$ (X=Ti, V, Cr, Mn, Fe, Co and Cu): the magnetic effect on the electron transport properties

1989 J. Phys.: Condens. Matter 1 1831

(http://iopscience.iop.org/0953-8984/1/10/004)

J. Phys.: Condens. Matter 1 (1989) 1831–1842. Printed in the UK

Electron transport properties of ternary metallic glasses $(Ni_{33}Zr_{67})_{1-x}X_x$ (X = Ti, V, Cr, Mn, Fe, Co and Cu): the magnetic effect on the electron transport properties

U Mizutani†, C Mishima† and T Goto‡

† Department of Crystalline Materials Science, Nagoya University, Furo-cho, Chikusa-ku, Nagoya 464, Japan

‡ The Institute for Solid State Physics, The University of Tokyo, Roppongi, Minato-ku, Tokyo 196, Japan

Received 13 July 1988

Abstract. The electrical resistivity has been measured in the temperature range 1.5–300 K for a large number of ternary metallic glasses $(Ni_{33}Zr_{67})_{1-x}X_x$ with X = Ti, V, Cr, Mn, Fe, Co and Cu. Its composition and temperature dependences are analysed. The characteristic features of the electron transport properties can be well extracted by taking the temperature derivative of conductivity. It turned out that the non-magnetic and non-superconducting metallic glasses form a universal master curve of $d\sigma/dT$ versus T, regardless of the atomic species of the third element X. Utilising this master curve as a reference, we could successfully single out the magnetic and superconducting contributions from the observed electron transport below about 300 K. We also found that the magnetic effect changes the square-root temperature dependence of conductivity below 15 K to a logarithmic one in both Cr and Mn alloy systems.

1. Introduction

Stable ternary metallic glasses can be formed by adding a variety of third elements to binary metal–metal amorphous alloys. The effect of the third element X on the electronic structure and electron transport of the non-magnetic metallic glass $Ni_{33}Zr_{67}$ has been extensively studied through the measurements of the electronic specific heat, the soft x-ray and photoemission spectroscopies (Yamada *et al* 1987a, b, 1988, Zehringer *et al* 1988a, b). The ternary alloy systems $(Ni_{33}Zr_{67})_{1-x}X_x$ so far studied may be conveniently divided into two families, one containing a light element like H, B, Al and Si and the other containing a 3d transition-metal element from Ti to Cu. It was shown that the light elements H, B and Si tend to form preferential bonding states with Zr atoms whereas Al and all 3d transition-metal elements interact more or less equally with host elements Zr and Ni. Another interesting point to be noted is that the ternary alloys containing the light element are non-magnetic but those containing the 3d transition-metal element, particularly Cr, Mn and Fe, yield the complex magnetic states.

The analysis of the electron transport properties of ternary metallic glasses $(Ni_{33}Zr_{67})_{1-x}X_x$ with light elements X = H, B, Al and Si has been made with the assumption that the ordinary conductivity formula $\sigma = (\frac{1}{3})e^2\Lambda_F v_F N(E_F)$ is applicable (Yamada *et al* 1987b). The assumption may well be justified in the non-magnetic system,

0953-8984/89/101831 + 12 $02.50

regardless of whether the Boltzmann-type ordinary transport mechanism dominates or competes with the quantum corrections such as the weak localisation and the electron–electron interaction. The situation ought to be more complicated when the 3d transition-metal element is employed as a third element. Here the magnetic interaction is likely to be superimposed. In the present work, we report the detailed analysis of the temperature dependence of the electrical resistivity for a large number of ternary metallic glasses $(Ni_{33}Zr_{67})_{1-x}X_x$ containing a 3d transition-metal element X from Ti to Cu and point out how magnetic effect perturbs the electron transport properties below 300 K.

2. Experimental procedure and results

Alloy ingots of the form $(Ni_{33}Zr_{67})_{1-x}X_x$ were prepared by arc melting appropriate amounts of constituent elements: Ni (99.97%), Zr (99.5%), Ti (99.7%), V (99.7%), Cr (99.99%), Mn (99.9%), Fe (99.9%), Co (99.9%) and Cu (99.99%). Amorphous ribbons were prepared using a single-roll spinning wheel apparatus in a reduced argon atmosphere. The formation of an amorphous phase was confirmed by x-ray diffraction with Cu Kα radiation. An amorphous single phase was relatively easily fabricated over the composition range of X up to $x = 0.3$ in every system.

The electrical resistivity was measured over the range 1.5–300 K using a four-probe DC method. The AC magnetic susceptibility was measured in a field amplitude of 10 Oe with 80 Hz in the temperature range 4.2–150 K. The DC magnetic susceptibility was also measured in the field of 1 T over the range 4.2–300 K.

Figures 1(*a*)–(*g*) show the temperature dependence of the electrical resistivity normalised with respect to that at 273 K for seven different alloy systems, together with the composition dependence of the resistivity at 300 K in each inset.

The temperature dependence of the magnetic susceptibility is fitted to the Curie–Weiss equation:

$$\chi = C/(T - \theta_p) \tag{1}$$

where C is the Curie constant and θ_p is the paramagnetic Curie temperature. The spin-freezing temperature T_f is deduced from the cusp in the AC magnetic susceptibility data.

Relevant numerical data are summarised in table 1.

3. Discussion

3.1. Resistivity versus carrier density at the Fermi level

Mizutani (1988a,b) pointed out that the metallic glasses containing appreciable amounts of d electrons at the Fermi level possess a possible minimum mean free path Λ_F limited by an average atomic distance and a reduced Fermi velocity v_F and, as a result, the conductivity formula $\sigma = (\frac{1}{3})e^2\Lambda_F v_F N(E_F)$ leads to an inversely proportional relationship between the resistivity and the number of total carriers at the Fermi level E_F. Indeed, the data of the resistivity versus the measured electronic specific heat coefficient γ fall on a hyperbolic curve for non-magnetic metallic glases, whose ρ–T curve is characterised by the exponential form over the wide temperature range below 300 K (Mizutani 1988b). This was taken as evidence for the validity of the conductivity formula with an almost constant factor $(\frac{1}{3})e^2\Lambda_F v_F$ in the high-resistivity limit.

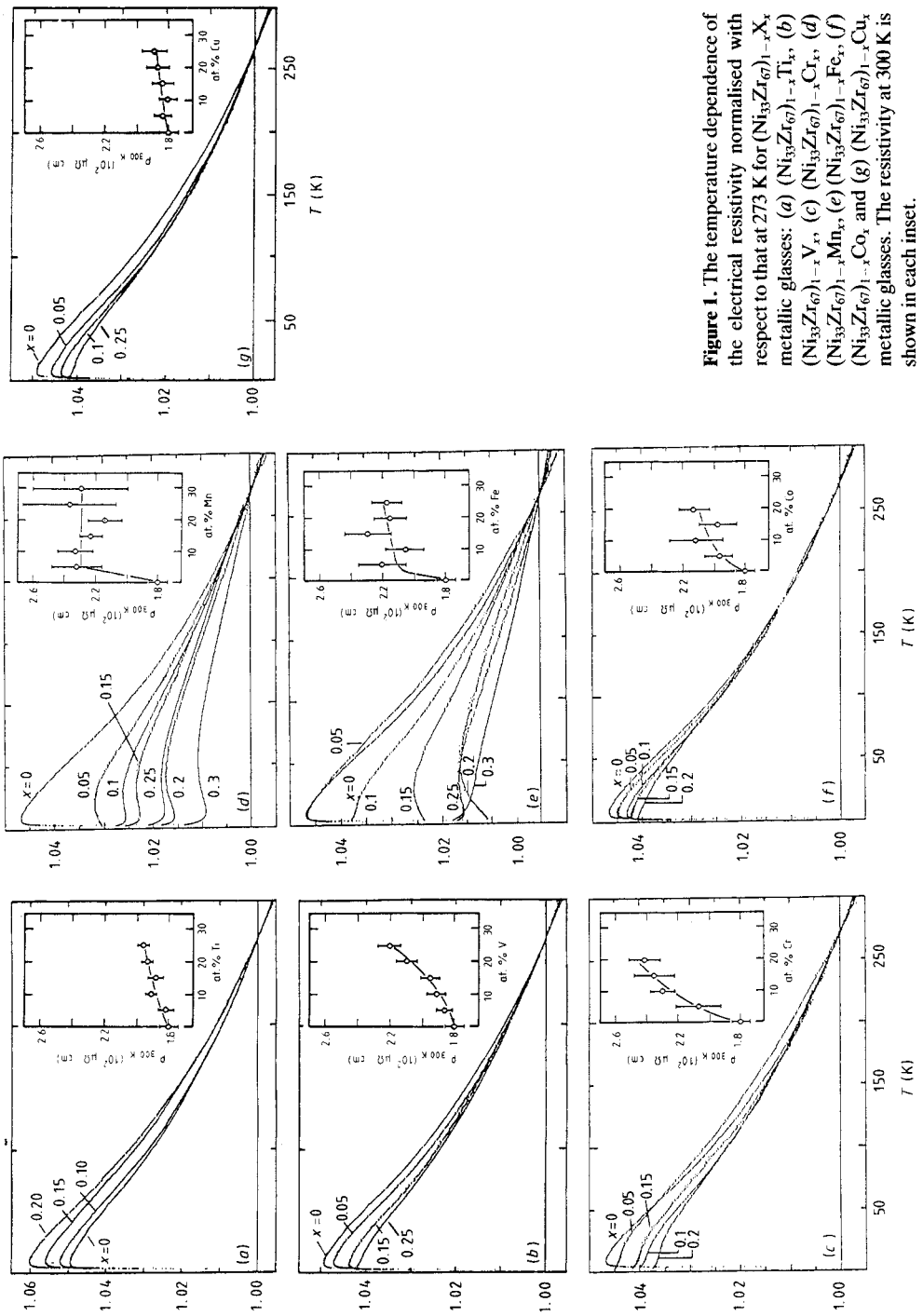

Figure 1. The temperature dependence of the electrical resistivity normalised with respect to that at 273 K for $(Ni_{33}Zr_{67})_{1-x}X_x$ metallic glasses: (*a*) $(Ni_{33}Zr_{67})_{1-x}Ti_x$, (*b*) $(Ni_{33}Zr_{67})_{1-x}V_x$, (*c*) $(Ni_{33}Zr_{67})_{1-x}Cr_x$, (*d*) $(Ni_{33}Zr_{67})_{1-x}Mn_x$, (*e*) $(Ni_{33}Zr_{67})_{1-x}Fe_x$, (*f*) $(Ni_{33}Zr_{67})_{1-x}Co_x$ and (*g*) $(Ni_{33}Zr_{67})_{1-x}Cu_x$ metallic glasses. The resistivity at 300 K is shown in each inset.

Table 1. Electron transport and magnetic properties of $(Ni_{33}Zr_{67})_{1-x}X_x$ metallic glasses. The value of Δ is determined by fitting the resistivity data in the range 30–300 K to the equation $\rho/\rho_0 = A + B\exp(-T/\Delta)$. Values of T_c in the brackets are derived from resistivity measurements. Otherwise, they are from the specific heat measurements (see Yamada *et al* 1988). The magnetic susceptibility χ for alloys with Ti, V and Cu is temperature independent and the value in the table refers to that at 300 K. The temperature dependent magnetic susceptibility in alloys with Cr, Mn and Fe is fitted to the equation $\chi = C/T - \theta_p$. The effective moment P_{eff} is calculated from the Curie constant C. The value of T_f refers to the spin freezing temperature determined by AC magnetic susceptibility measurements.

Sample	x	ρ_{300K} ($\mu\Omega$ cm)	Δ (K)	T_c (K)	$\chi_{4.2K}$ (10^{-4} emu mol^{-1})	C (10^{-4} emu K mol^{-1})	P_{eff} (μ_B)	θ_p (K)	T_f (K)
Ni–Zr–Ti	0.05	182 ± 5	223	2.73	1.22				
	0.10	191 ± 3	232	2.67	1.31				
	0.15	188 ± 5	276	2.65	1.33				
	0.20	193 ± 4	244	2.60	1.38				
	0.25	196 ± 4	269	2.58	1.42				
Ni–Zr–V	0.05	184 ± 6	216	2.25	1.26				
	0.10	181 ± 6	215	2.08					
	0.15	184 ± 7	227	1.79	1.36				
	0.20	187 ± 7	233		1.45				
	0.25	189 ± 8	257		1.50				
Ni–Zr–Cr	0.05	207 ± 14			0.81				
	0.10	230 ± 8							
	0.15	235 ± 13			1.83	7.58	0.20	−2.3	
	0.20	241 ± 10			47.2				
Ni–Zr–Mn	0.05	232 ± 14			8.23	52	0.91	−3.2	
	0.10	233 ± 11			14.9	99	0.89	−3.3	
	0.15	223 ± 7			24.9	194	1.02	−4.1	
	0.20	214 ± 11			20.3	153	0.78	−4.1	
	0.25	237 ± 30			25.1	200	0.80	−5.1	
	0.30	229 ± 30			18.7	141	0.61	−5.1	
Ni–Zr–Fe	0.05	220 ± 15		1.70					
	0.10	205 ± 14		(2.0)	1.64				
	0.15	229 ± 15		(2.0)	3.92	115	0.78	−54	
	0.20	215 ± 10			87.6	1160	2.15	2.3	
	0.25	217 ± 10			294	3110	3.15	73	12.5
	0.30	286 ± 26			979				54
Ni–Zr–Co	0.05	197 ± 9	217	2.40					
	0.10	212 ± 17	233	2.10					
	0.15	198 ± 12	249		1·03				
	0.20	213 ± 10			2.27				
Ni–Zr–Cu	0.05	186 ± 5	229	2.43	1.09				
	0.10	191 ± 6	263	2.07	1.05				
	0.15	195 ± 6	243	1.87	0.97				
	0.20	210 ± 6	269		0.92				
	0.25	221 ± 7	238		0.84				

The ρ versus γ plot becomes less clear for the magnetic metallic glasses, since the measured T-linear specific heat coefficient is heavily perturbed by the magnetic effect and no longer represents the density of states at E_F. To see this effect more clearly, we calculated from insets in figure 1 the derivative of the resistivity with respect to the composition of X for all alloy systems studied. The value is also calculated for alloys containing light elements (Yamada *et al* 1987b). Figure 2 shows the resulting value as a

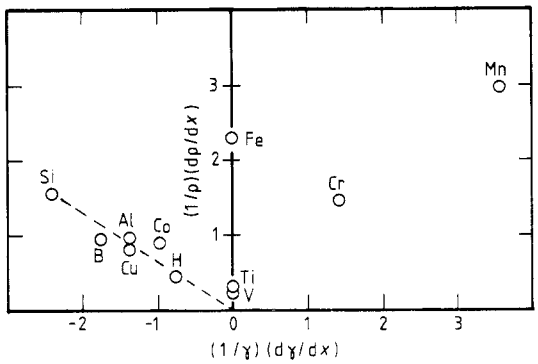

Figure 2. The normalised composition derivative of resistivity at 300 K against the normalised composition derivative of the electronic specific heat coefficient γ for $(Ni_{33}Zr_{67})_{1-x}X_x$ metallic glasses with X = H, B, Al, Si, Ti, V, Cr, Mn, Fe, Co and Cu.

function of the corresponding derivative of the electronic specific heat coefficient, which has been already reported elsewhere (Yamada *et al* 1987a, 1988). The value of $d\rho/dx$ is found to be positive for all systems. The value of $d\gamma/dx$ is negative and fits well to an almost straight line for alloys containing H, B, Al, Si, Ti, V, Co and Cu. This is consistent with the above-mentioned finding that an increase in ρ is caused by a decrease in γ. We consider this to be a characteristic feature of high-resistivity non-magnetic metallic glasses.

The value of $d\gamma/dx$ for alloys with Cr and Mn is large and positive. This originates from the fact that the measured value of γ is enhanced beyond the band structure contribution due to the magnetic effect. The value of $d\rho/dx$ is found to be also unusually large, as compared with those for non-magnetic alloy systems discussed above. The data for the Fe alloys are further unusual: the value of $d\rho/dx$ is positive and large in spite of a vanishingly small value of $d\gamma/dx$. As reported earlier (Yamada *et al* 1988), the 5 at.% Fe alloy is evidenced from the specific heat measurement to be superconductor with T_c of 1.7 K. Furthermore, the value of γ retains essentially the same value as that of the host binary alloy $Ni_{33}Zr_{67}$ up to $x = 0.15$, leading to $d\gamma/dx = 0$. Nevertheless, the magnetic susceptibility becomes definitely temperature dependent when x exceeds 0.1. As will be mentioned later, a trace of superconductivity is observed in the temperature dependence of the conductivity for alloys up to $x = 0.15$, though the specific heat data no longer indicate a jump associated with the superconducting transition for alloys with $x \geqslant 0.1$. An apparent coexistence of superconductivity and magnetism is most likely responsible for the unusual location of the data in figure 2. This unique property might be indicative of the presence of unavoidable heterogeneous distribution of Fe atoms in the matrix.

The composition dependence of the superconducting transition temperature T_c can also be used as a measure to see how the magnetic effect participates with increasing X concentration. The value of T_c in the present resistivity measurements can be detected down to 1.5 K. As listed in table 1, the superconductivity disappears even at the least concentration of $x = 0.05$ for Cr and Mn alloy systems, indicating that these two elements exert the strongest magnetic effect. On the other hand, a decreasing rate in T_c with increasing the X concentration is the least in the Ti alloys and moderate in the V and Cu alloy systems, the latter being comparable to that in the Al alloys reported earlier (Yamada *et al* 1987a, b). This may be characteristic of a non-magnetic system. The value

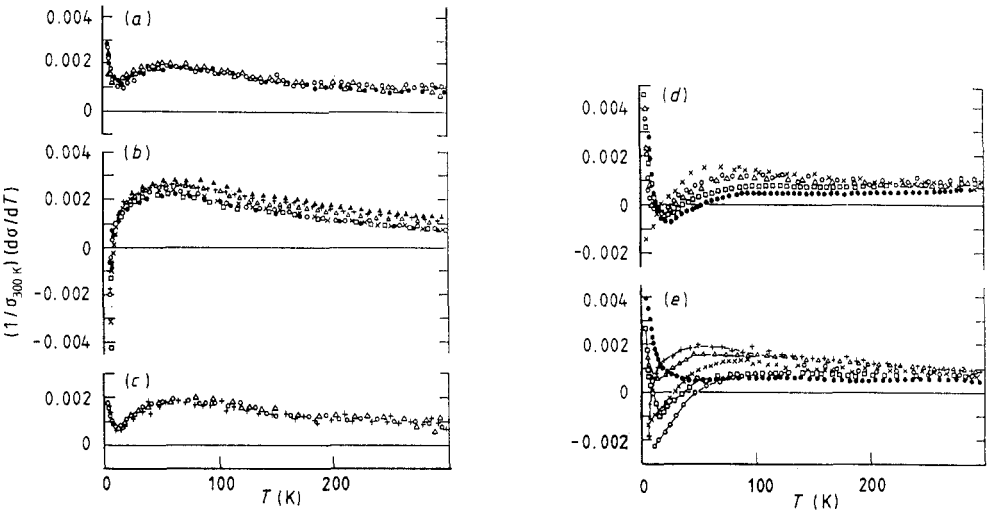

Figure 3. The normalised temperature derivative of conductivity against temperature for $(Ni_{33}Zr_{67})_{1-x}X_x$ metallic glasses: (*a*) non-magnetic and non-superconducting metallic glasses, ○: $Al_{0.3}$, ●: $Si_{0.2}$ and △: $Cu_{0.25}$; (*b*) superconducting metallic glasses, ×: $Ni_{33}Zr_{67}$, ○: $Cu_{0.15}$, □: $Co_{0.1}$, ●: $V_{0.15}$, △: $Ti_{0.1}$, +: $Ti_{0.15}$ and ▲: $Ti_{0.2}$; (*c*) Cr–metallic glasses, △: $Cr_{0.05}$, ○: $Cr_{0.1}$ and +: $Cr_{0.2}$; (*d*) Mn–metallic glasses, ×: $Mn_{0.05}$, ○: $Mn_{0.1}$, △: $Mn_{0.15}$, □: $Mn_{0.25}$ and ●: $Mn_{0.3}$; and (*e*) Fe–metallic glasses, +: $Fe_{0.05}$, △: $Fe_{0.1}$, ×: $Fe_{0.15}$, ○: $Fe_{0.2}$, □: $Fe_{0.25}$ and ●: $Fe_{0.3}$.

of T_c in the Co alloy system is suppressed below 1.5 K only when its content exceeds 0.15. This fact, along with the composition dependence of the electronic specific heat coefficient (Yamada *et al* 1988) and the analysis based on figure 2, persuades us to believe that the Co alloys are regarded as non-magnetic, at least, in the composition range $x \leqslant 0.2$ studied in the present work. From the above discussion, we conclude that all alloys with Cr and Mn and alloys with Fe content of $x \geqslant 0.1$ are magnetic and the rest of alloys containing Ti, V, Co and Cu are non-magnetic.

3.2. Magnetic effect in the ρ–T characteristics

In the high-resistivity metallic glasses, one has been well aware that quantum corrections are of prime importance in determining the temperature dependence of resistivity. In the low-temperature regime, below about 15 K, the square-root temperature dependence has been observed in non-magnetic metallic glasses and attributed to the electron–electron interaction (Mizutani *et al* 1988b). At higher temperatures, 30–300 K, the ρ–T characteristics of high-resistivity non-magnetic metallic glasses can be empirically well expressed by an exponential function $\rho/\rho_0 = A + B\exp(-T/\Delta)$, where the parameter Δ represents the characteristic temperature. This unique temperature dependence cannot be explained within the context of the ordinary Boltzmann-type scattering mechanism and has been ascribed to the delocalisation process assisted by phonons (Mizutani 1988a, b). We may hereafter use the conductivity rather than the resistivity to discuss the scattering mechanism in such high-resistivity alloys.

Pureur *et al* (1988) employed the temperature derivative of the resistivity for the magnetic metallic glass $Fe_{0.92}Zr_{0.08}$ to ease the location of the magnetic transition point in the ρ–T curve. Similarly, we plotted in figure 3 the temperature derivative of the

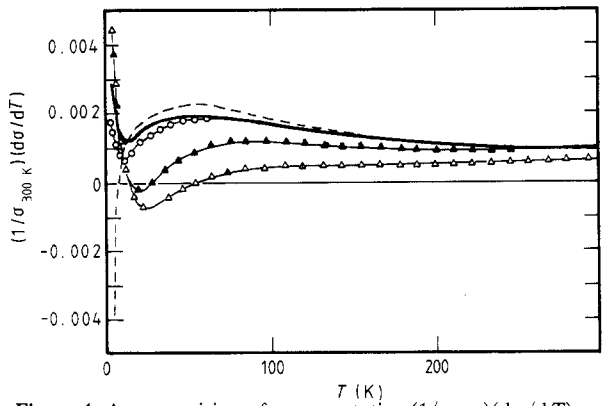

Figure 4. A comparision of representative $(1/\sigma_{300\,K})(d\sigma/dT)$ versus temperature curves in $(Ni_{33}Zr_{67})_{1-x}X_x$ metallic glasses. ——: non-magnetic and non-superconducting master curve derived from figure 3, – – –: curve for superconducting alloys, –○–○–: curve for Cr alloys, –▲–▲–: curve for 10 at.% Mn alloy and –△–△–: curve for 30 at.% Mn alloy.

conductivity against temperature for various metallic glasses $(Ni_{33}Zr_{67})_{1-x}X_x$ studied in this and previous experiments. The data for three different non-magnetic and non-superconducting metallic glasses are shown in figure 3(*a*). All of them are found to fall on a master curve, regardless of the atomic species of a third element. As will be shown later, a steep increase in the $d\sigma/dT$ curve at the lowest temperature region is well expressed by the square-root temperature dependence of the conductivity. The slowly decreasing slope of the $d\sigma/dT$ curve above about 50 K corresponds to the exponential-type temperature dependence in the resistivity expression mentioned above.

The $d\sigma/dT$ data for superconducting alloys and magnetic systems containing Cr, Mn and Fe are shown in figure 3(*b*)-(*e*), respectively. To allow a direct comparison with the non-magnetic master curve, representative $d\sigma/dT$ curves for the respective groups are redrawn in figure 4 relative to the master curve in figure 3(*a*). The data for superconducting alloys also fall almost on a single curve, although the data for the Ti alloys tend to deviate consistently upwards. The representative curve for the superconducting alloys is indicated by a broken curve in figure 4. The deviation from the non-magnetic master curve becomes evident below about 150 K. The superconducting fluctuations are known to persist up to about 30 K in these metallic glass systems (Toyota *et al* 1984). The observed deviation in $d\sigma/dT$ occurring at an unexpectedly high temperature may be considered as a precursory effect associated with the superconducting fluctuations.

The data for the Cr alloys shown in figure 3(*c*) are apparently identical to the non-magnetic master curve. However, the minimum in $d\sigma/dT$ near 10 K is deeper than the master curve, as is clearly seen in figure 4. It is also found that the deviation from the non-magnetic master curve becomes noticeable below about 30 K. The DC magnetic susceptibility was measured for the 15 at.% Cr alloy and it turned out that the weak Curie–Weiss-type temperature dependence is observed below about 50 K. As listed in table 1, the paramagnetic Curie temperature is negative and the effective moment deduced from the Curie constant is only $0.2\mu_B$. Therefore, it is clear that even a small effective magnetic moment is strong enough to cause the magnetic perturbation in the electron transport properties of the Cr alloy system.

The data for the Mn alloys in figure 3(*d*) no longer fall on a single curve but depend sensitively on Mn concentration. Except for the 5 at.% Mn data all curves are found to

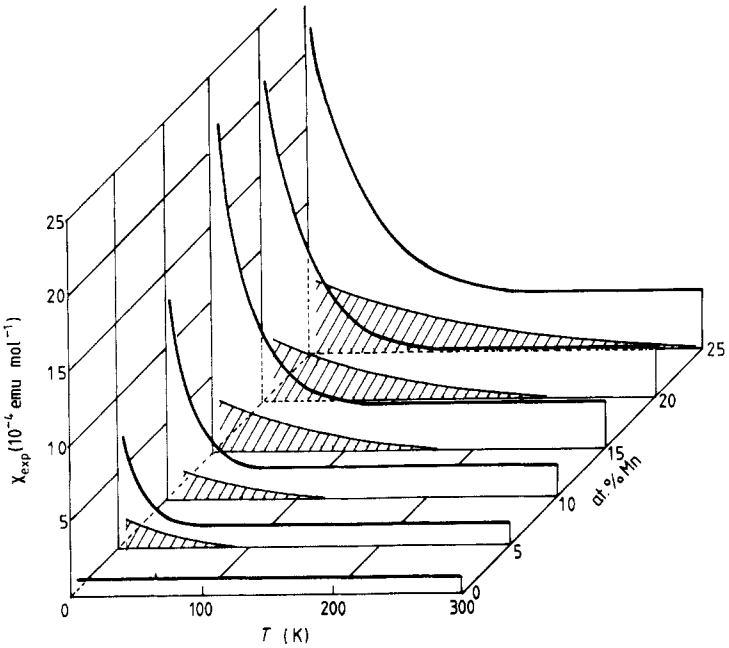

Figure 5. The temperature dependence of DC magnetic susceptibility for $(Ni_{33}Zr_{67})_{1-x}Mn_x$ metallic glasses. The shaded area shows schematically the magnetic contribution to the temperature dependence of conductivity.

intersect the temperature axis twice, corresponding to the resistivity maximum and minimum in figure 1(*d*). As illustrated in figure 4, the data may be viewed such that the magnetic interaction in Mn alloys is further enhanced beyond that in the Cr alloys and brings further the $d\sigma/dT$ curve downwards to intersect with the temperature axis. A comparison with the non-magnetic master curve clearly indicates that the magnetic effect persists up to above 200 K in dilute Mn alloys and to above 300 K in concentrated alloys.

As shown in figure 3(*e*), the $d\sigma/dT$ curve for the Fe alloy system changes quite drastically with increasing Fe concentration. This suggets that the magnetic state also changes in a complicated manner with increasing Fe concentration. Hence, further detailed analysis based on magnetic data is needed, particularly, for the Mn and Fe alloy systems, where the magnetic state varies dramatically as a function of X concentration. This is described in the next section.

3.3. Magnetic states in Mn and Fe alloy systems

Figure 5 illustrates the DC magnetic susceptibility against temperature and the composition of the third elements Mn. The data in the temperature range 4.2–150 K for the Mn alloys are fitted to the Curie–Weiss equation (1). The Curie temperature and the effective moment thus deduced are summarised in table 1. A negative Curie temperature indicates that the Mn atoms interact with each other antiferromagnetically. The magnetic susceptibility at 300 K and the Curie temperature increases, but the effective moment slightly decreases with increasing Mn content. The deviation of the $d\sigma/dT$ curve from the non-magnetic master curve is schematically incorporated in figure 5. It is clear that

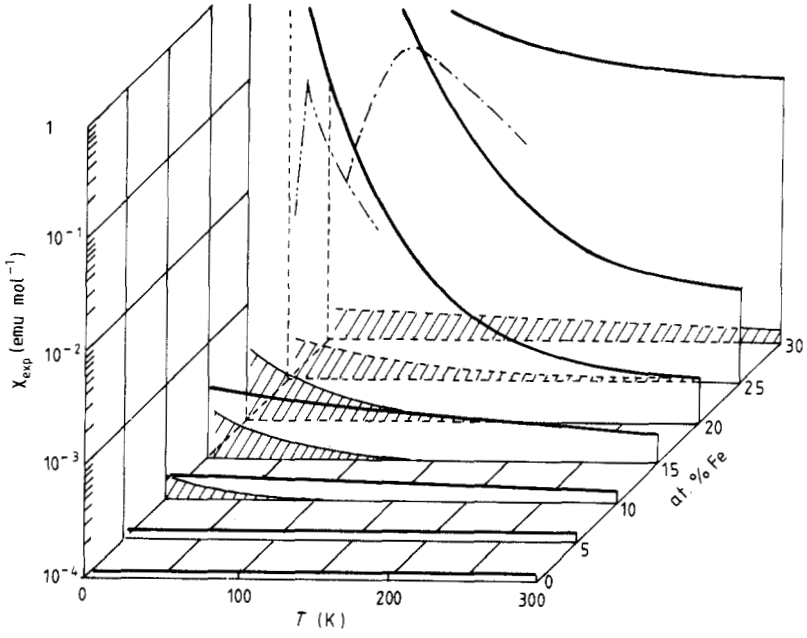

Figure 6. The temperature dependence of DC magnetic susceptibility for $(Ni_{33}Zr_{67})_{1-x}Fe_x$ metallic glasses. The shaded area shows schematically the magnetic contribution to the temperature dependence of conductivity. The chain curve shows the temperature dependence of the AC magnetic susceptibility on an arbitrary scale for 25 and 30 at.% Fe alloys.

the magnetic contribution to the electron transport appears at low temperatures and extends to higher temperatures with increasing magnetic interaction.

The temperature dependence of the DC magnetic susceptibility for the Fe alloy system is shown in figure 6. The temperature dependence appears as the Fe content reaches 10 at.% and further increase in Fe content changes drastically its magnitude (note the logarithmic scale here in contrast to the ordianry scale in figure 5). The AC magnetic susceptibility data are also incorporated in figure 6 as a chain line for the 25 and 30 at.% Fe alloys. The presence of the cusp in the AC magnetic susceptibility indicates the transition to the spin-glass state at lower temperatures. The magnetic contribution to the conductivity estimated from the $d\sigma/dT$ curve is also illustrated in figure 6 to allow a direct comparison with the magnetic data. Again, the magnetic effect on the electron transport develops first at low temperatures and extends its region to higher temperatures with increasing magnetic interaction.

3.4. Temperature dependence of conductivity at lowest temperatures

Cochrane and Strom-Olsen (1984) analysed the observed square-root temperature dependence of the conductivity in various metallic glasses and proposed the existence of the scaling behaviour between its temperature coefficient and the magnitude of the resistivity, regardless of the magnetic state involved. As already discussed, however, we found that the rising slope of $d\sigma/dT$ below about 10 K in magnetic systems is substantially different from that in the non-magnetic master curve. Hence, it seems natural to expect the different temperature dependences of conductivity at low temperatures, depending on whether the system is magnetic or non-magnetic.

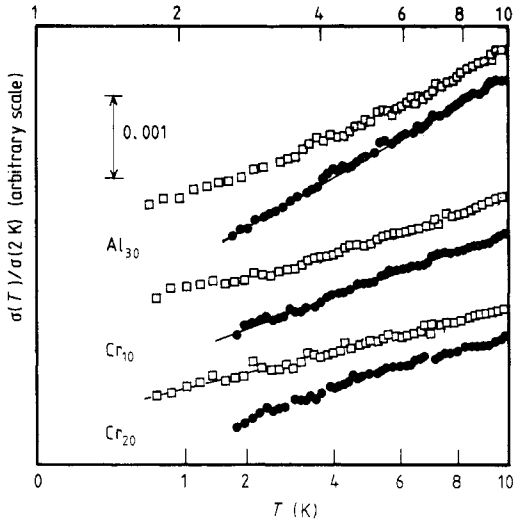

Figure 7. The temperature dependence of low-temperature conductivity normalised with respect to that at 2 K on both square-root (full circles) and logarithmic (open squares) scales for $(Ni_{33}Zr_{67})_{70}Al_{30}$, $(Ni_{33}Zr_{67})_{90}Cr_{10}$ and $(Ni_{33}Zr_{67})_{80}Cr_{20}$ metallic glasses.

Figure 7 shows both logarithmic and square-root temperature dependences of the conductivity for one of the non-magnetic and non-superconducting metallic glasses, $(Ni_{33}Zr_{67})_{70}Al_{30}$, together with those for Cr alloys. The validity of the square-root temperature dependence can be confirmed. This holds true in other non-magnetic and non-superconducting $(Ni_{33}Zr_{67})_{1-x}X_x$ metallic glasses containing H, B, Si, Cu and so on. However, as is seen in figure 7, the logarithmic temperature dependence seems to become a better expression in the Cr alloy system when its content reaches 20 at.%. This suggests that the introduction of the magnetic effect changes the square-root temperature dependence to the logarithmic one in the low-temperature σ–T characteristics.

The data for the Mn alloys are shown in figure 8. The logarithmic temperature dependence is again better fitted to the experimental data, though its applicable range is limited below about 5 K. The data for the Fe alloys are shown in figure 9. The alloy with 10 at.% Fe apparently undergoes the superconducting transition at about 2 K, though the magnetic susceptibility already shows a weak temperature dependence over a wide temperature range (see figure 6). In the case of the Fe alloy sytem it seems that a linear fitting is rather poor on both the square-root and logarithmic temperature scales even below about 4 K. The measurements below 1.5 K may be needed. In spite of uncertainties in the Fe alloy system, we believe that an increase in magnetic interactions destroys the square-root temperature dependence in the non-magnetic and non-superconducting $(Ni_{33}Zr_{67})_{1-x}X_x$ metallic glasses and that the logarithmic temperature dependence becomes a better expression, particularly, in the Cr and Mn alloy systems.

Finally, we plotted in figure 10 the slope of the σ versus $\sqrt{T}$ curve below 10 K as a function of the resistivity at 300 K for non-magnetic and non-superconducting metallic glasses $(Ni_{33}Zr_{67})_{1-x}X_x$ so far studied, together with the data for the Ag–Cu–Ge metallic glasses recently studied (Mizutani *et al* 1988). Note here the difference in the electronic structure between them: the former possesses an appreciable number of d electrons at the Fermi level whereas the latter has exclusively sp electrons. Although a more or less quadratic relation holds, the data for respective alloy groups fall on entirely different

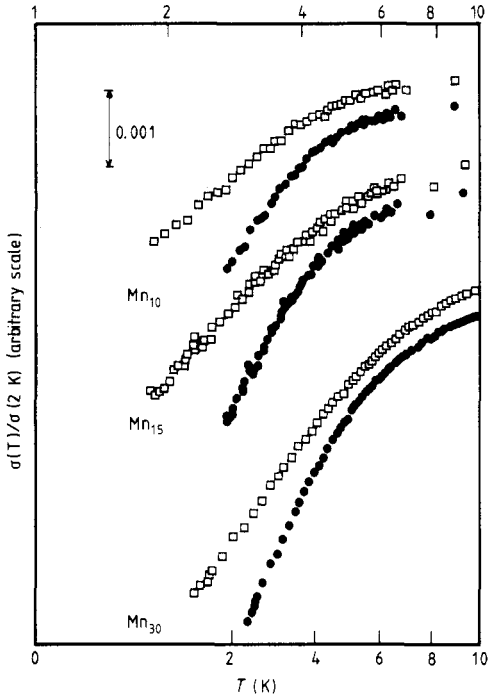

Figure 8. The temperature dependence of low-temperature conductivity normalised with respect to that at 2 K on both square-root (full circles) and logarithmic (open squares) scales for $(Ni_{33}Zr_{67})_{1-x}Mn_x$ metallic glasses with $x = 0.1$, 0.15 and 0.3.

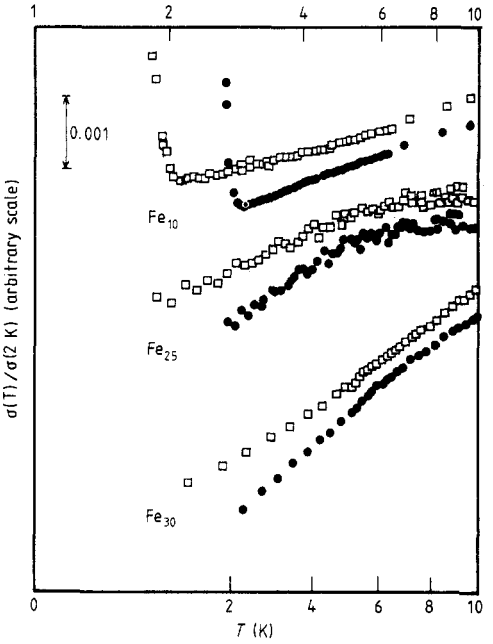

Figure 9. The temperature dependnece of low-temperature conductivity normalised with respect to that at 2 K on both square-root (full circles) and logarithmic (open squares) scales for $(Ni_{33}Zr_{67})_{1-x}Fe_x$ metallic glasses with $x = 0.1$, 0.25 and 0.3. A sharp increase in conductivity for the alloy with $x = 0.1$ may be due to the superconducting transition. A similar sharp increase at nearly the same temperature is observed for the alloy with $x = 0.15$.

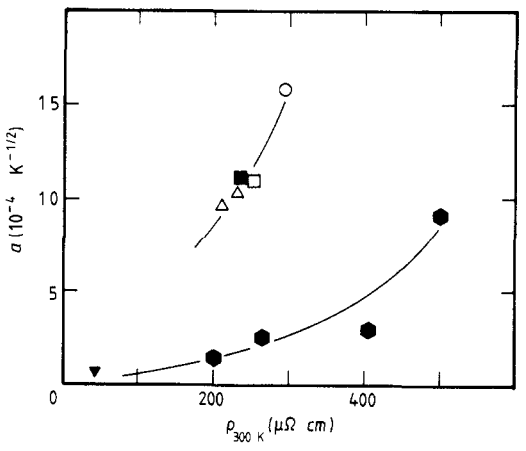

Figure 10. The square-root coefficient A against the resistivity for non-magnetic and non-superconducting metallic glasses. The coefficient A is determined by fitting the conductivity σ below 10 K to the expression $\sigma(T) = \sigma(0)[1 + A\sqrt{T}]$. Symbols used are as follows; ○: $(Ni_{33}Zr_{67})H_{1.18}$, □: $(Ni_{33}Zr_{67})_{75}Si_{25}$ and $(Ni_{33}Zr_{67})_{80}Si_{20}$, ●: $(Ni_{33}Zr_{67})_{75}B_{25}$, △: $(Ni_{33}Zr_{67})_{70}Al_{30}$ and $(Ni_{33}Zr_{67})_{75}Al_{25}$ (Yamada *et al* 1987b), ⬢: $(Ag_{0.5}Cu_{0.5})_{1-x}Ge_x$ (Mizutani *et al* 1988) and ▼: Mg–Zn (Matsuda and Mizutani 1982). An upward deviation in resistivity for low-resistivity metallic glasses like Mg–Zn has been observed below about 10 K. Because of its small magnitude, it is difficult to identify its temperature dependence. Here we determined the coefficient A by assuming the validity of the above equation even for such a low-resistivity alloy.

curves. This indicates the lack of a universal relationship between the square-root coefficient and the resistivity. Mizutani (1988b) pointed out that the quantum corrections to the conductivity in sp-electron metallic glasses become comparable to those in d-electron metallic alloys, only when the resistivity exceeds about 500 $\mu\Omega$ cm in the former. This conclusion is consistent with the data in figure 10: the square-root coefficient in the Ag–Cu–Ge metallic glasses reaches more or less the same value as that in $(Ni_{33}Zr_{67})_{1-x}X_x$ metallic glasses, when the resistivity reaches the value of 500 $\mu\Omega$ cm.

Acknowledgment

We are grateful to Dr Y Yamada and Mr Y Itoh for their assistance and helpful discussions at the early stage of this work.

References

Cochrane R W and Strom-Olsen J O 1984 *Phys. Rev.* B **29** 1088
Matsuda T and Mizutani U 1982 *J. Phys. F: Met. Phys.* **12** 1877
Mizutani U 1988a *Mater. Sci. Eng.* **99** 165
—— 1988b *Trans. Japan. Inst. Met. Suppl.* **29** 275
Mizutani U, Sato K, Sakamoto I and Yonemitsu K 1988 *J. Phys. F: Met. Phys.* **18** 1995
Pureur P, Schreiner W H and Kunzler J V, Ryan D H and Coey J M D 1988 *Solid State Commun.* **65** 163
Toyota N, Inoue A, Matsuzaki K, Fukase T and Masumoto T 1984 *J. Phys. Soc. Japan* **53** 924
Yamada Y, Itoh Y, Matsuda T and Mizutani U 1987b *J. Phys. F: Met. Phys.* **17** 2313
Yamada Y, Itoh Y, Mizutani U, Shibagaki N and Tanaka K 1987a *J. Phys. F: Met. Phys.* **17** 2303
Yamada Y, Itoh Y and Mizutani U 1988 *Mater. Sci. Eng.* **99** 289
Zehringer R, Oelhafen P, Güntherodt H-J, Yamada Y and Mizutani U 1988a *Mater. Sci. Eng.* **99** 253
—— 1988b *Mater. Sci. Eng.* **99** 317